Avinash Kumar Agarwal[1]
Engine Research Laboratory,
Department of Mechanical Engineering,
Indian Institute of Technology Kanpur,
Kanpur 208016, India
e-mail: akag@iitk.ac.in

Nikhil Sharma
Engine Research Laboratory,
Department of Mechanical Engineering,
Indian Institute of Technology Kanpur,
Kanpur 208016, India
e-mail: nikhil5461@gmail.com

Akhilendra Pratap Singh
Engine Research Laboratory,
Department of Mechanical Engineering,
Indian Institute of Technology Kanpur,
Kanpur 208016, India
e-mail: akhips@iitk.ac.in

Vikram Kumar
Engine Research Laboratory,
Department of Mechanical Engineering,
Indian Institute of Technology Kanpur,
Kanpur 208016, India
e-mail: vikramk@iitk.ac.in

Dev Prakash Satsangi
Engine Research Laboratory,
Department of Mechanical Engineering,
Indian Institute of Technology Kanpur,
Kanpur 208016, India
e-mail: devprakashsatsangi2017@gmail.com

Chetankumar Patel
Engine Research Laboratory,
Department of Mechanical Engineering,
Indian Institute of Technology Kanpur,
Kanpur 208016, India
e-mail: chetanpatel.iitk@gmail.com

Adaptation of Methanol–Dodecanol–Diesel Blend in Diesel Genset Engine

Miscibility of methanol in mineral diesel and stability of methanol–diesel blends are the main obstacles faced in the utilization of methanol in compression ignition engines. In this experimental study, combustion, performance, emissions, and particulate characteristics of a single-cylinder engine fueled with MD10 (10% v/v methanol blended with 90% v/v mineral diesel) and MD15 (15% v/v methanol blended with 85% v/v mineral diesel) are compared with baseline mineral diesel using a fuel additive (1-dodecanol). The results indicated that methanol blending with mineral diesel resulted in superior combustion, performance, and emission characteristics compared with baseline mineral diesel. MD15 emitted lesser number of particulates and NO_x emissions compared with MD10 and mineral diesel. This investigation demonstrated that methanol–diesel blends stabilized using suitable additives can resolve several issues of diesel engines, improve their thermal efficiency, and reduce NOx and particulate emissions simultaneously. [DOI: 10.1115/1.4043390]

Keywords: methanol, combustion, diesel–methanol blends, emissions, particulates

1 Introduction

Increasing global population and growing urbanization have imposed heavy demand on the transport sector. International Energy Agency (IEA) predicted a significant increase (~50%) from current levels in the global transport energy usage by 2030, which may possibly double by 2050 [1]. Presently, most energy is supplied by fossil fuels and a small fraction of energy is supplied by renewable energy sources [2]. Pollutants emitted from these fossil-fuel powered engines pose yet another important concern, which needs immediate attention. To combat these twin issues, researchers have proposed solutions such as the use of after-treatment devices, advanced combustion strategies, and alternative fuels [3]. Hydrogen, natural gas, biofuels, and alcohols are important alternative fuels, which have been explored for engine applications [4]. The presence of additional oxygen in molecules of alcohols improves their combustion characteristics, leading to lower emissions of particulate [5]. Among primary alcohols (methanol, ethanol, propanol, and butanol), methanol possesses the highest inherent fuel oxygen (50% w/w), which is an important factor for smoother engine combustion. Methanol can be produced from coal, natural gas, and biomass at a relatively lower cost compared to conventional fuels.

There are several methods to utilize methanol as a fuel in diesel engines such as fumigation, dual-fuel injection, blending, and emulsification [6,7]. Methanol's poor solubility in mineral diesel poses a big challenge for methanol utilization in CI engines using the blending technique. The dipole moment induced to nonpolar hydrocarbon backbone by the hydroxyl moiety present in alcohols makes them more polar and lowers the upper limit of blending in petroleum fuels without the use of a co-solvent [8]. Bayraktar [9] conducted experiments on a single-cylinder CI engine using diesel–methanol–dodecanol blends. He varied methanol concentration from 2.5% to 15% and performed experiments at different compression ratios (19, 21, 23, and 25). He observed ~7% improvement in engine performance with 10% methanol–diesel blend (MD10). Sayin et al. [10] used 5%, 10%, and 15% methanol–diesel blends in a CI engine and reported higher brake-specific fuel consumption (BSFC), and NOx emissions from methanol–diesel blends however brake thermal efficiency (BTE), smoke opacity, CO and

[1]Corresponding author.

Contributed by the Internal Combustion Engine Division of ASME for publication in the Journal of Energy Resources Technology. Manuscript received January 1, 2019; final manuscript received April 1, 2019; published online April 22, 2019. Assoc. Editor: Hameed Metghalchi.

HC decreased with increasing methanol blending in diesel. Yilmaz and Donaldson [11] used modeling to investigate chemical processes involved during combustion of methanol in a diesel engine. They observed that use of methanol in diesel engines leads to lower engine efficiency and higher emissions due to engine oil dilution with fuel. This may also lead to engine failure at higher engine load conditions. Jamkorzik [12] also performed engine experiments using methanol–diesel blends and reported lower CO emission and higher NOx emissions from methanol–diesel blends. He also reported that HC and CO_2 emissions were not affected significantly by addition of methanol in diesel. Canakci et al. [13] used different methanol–diesel blends ranging from 0% to 15% (v/v) of methanol. They observed an increase in BSFC with increasing methanol content in the blend. They also observed a reduction in CO, HC emissions but increases NOx emissions with increasing methanol percentage in methanol–diesel blends. Huang et al. [14] investigated the effect of oxygen on combustion characteristics when using different methanol–diesel blends (0% to ~14% (w/w) oxygen in steps of 2). They found that increasing methanol content in the test blend resulted in shorter combustion duration (CD) and higher heat release rate (HRR). Increasing methanol content in the test fuel also shifted the combustion more towards premixed combustion phase. Agarwal et al. [15] used methanol–diesel blend (MD5) to assess unregulated emissions from a diesel engine. They did not observe any significant change in unregulated emissions from MD5 compared with baseline mineral diesel. Another study by Wei et al. [16] revealed that increasing methanol content up to 30% (v/v) in mineral diesel did not affect unregulated emissions; however, CO, HC, and NOx emissions reduced. Wu et al. [17] optimized methanol energy-share ratio, fuel injection timing of methanol, and inlet air temperature using Taguchi methodology for a diesel/methanol blend fueled engine. They reported that diesel/methanol blend emitted lower smoke, CO, HC, and NOx emissions compared with baseline mineral diesel. Addition of methanol in mineral diesel also affected the combustion characteristics of the engine due to variations in fuel properties [18–20]. Addition of methanol in mineral diesel results in shorter combustion duration and higher HRR. Compression ratio and use of exhaust gas recirculation also affected the emissions of NOx, THC, and CO as well as performance characteristics of methanol-fueled engine [21].

In this study, two fuel blends of methanol (10% and 15% v/v) with remaining mineral diesel were investigated for engine performance, emissions, combustion, and particulate characteristics. In addition, the use of 1-dodecanol as a fuel additive to enhance fuel miscibility was explored and its effect on the engine characteristics was evaluated. In the end, a statistical analysis of particulate results based on particulate number–size distribution, surface area–size distribution, and mass–size distribution was performed. To emphasize the advantages of methanol addition on both particulate and NOx emissions, a NOx-PM analysis was also performed. The outcome of this experimental study can be directly implemented in the engines used in variety of applications such as agricultural pump sets, threshers, sugarcane crushers, rice hullers, coffee pulper, chaff cutter, flour mills, sawmills, sprinklers, oil expeller, water-pump set, power generation, concrete mixer, flour mills, sewage cleaning, as well as in marine applications.

2 Experimental Setup and Methodology

2.1 Fuel Preparation and Fuel Characterization. In this manuscript, the blends of alcohol and diesel are referred as "Diesohol" [5]. The phase separation issue was resolved by adding a suitable additive while blending. 1-Dodecanol is a fatty alcohol, which is typically produced from coconut [22]. 1-Dodecanol has almost similar calorific value as that of mineral diesel but has relatively higher viscosity and autoignition temperature [22]. In this experimental investigation, 1-dodecanol was used to avoid phase separation and to make stable methanol–diesel blends. Figure 1 shows the test blends in unstable (without 1-dodecanol) and stable (with 1-dodecanol) forms.

Important test fuel properties such as density, kinematic viscosity, and calorific value were measured using portable density meter (Kyoto Electronics; DA130N), kinematic viscometer (Stanhope-Seta; 83541-3), and bomb calorimeter (Parr; 6200), respectively. These properties will be helpful to discuss the results of this experimental study. Table 1 shows the composition of all test fuels and their important properties.

Fuel characterization results showed that increasing methanol content in the test blend reduced its calorific value and kinematic viscosity. The density of test fuels was not affected by the increasing fraction of methanol in the test fuels.

2.2 Experimental Setup and Test Matrix. The experiments were conducted using a production-grade single-cylinder, four-stroke, water-cooled, naturally aspirated, constant speed diesel

Table 1 Test fuels compositions and important fuel properties

Test fuel	Volumetric content (%, v/v)			Calorific value (MJ/kg)	Kinematic viscosity (mm^2/s) @ 40 °C	Density (g/cm^3) @ 30 °C
	Diesel	Methanol	1-dodecanol			
Diesel	100	—	—	44.26	2.92	0.837
MD10	89	10	1	43.12	2.81	0.829
MD15	84	15	1	42.31	2.69	0.825

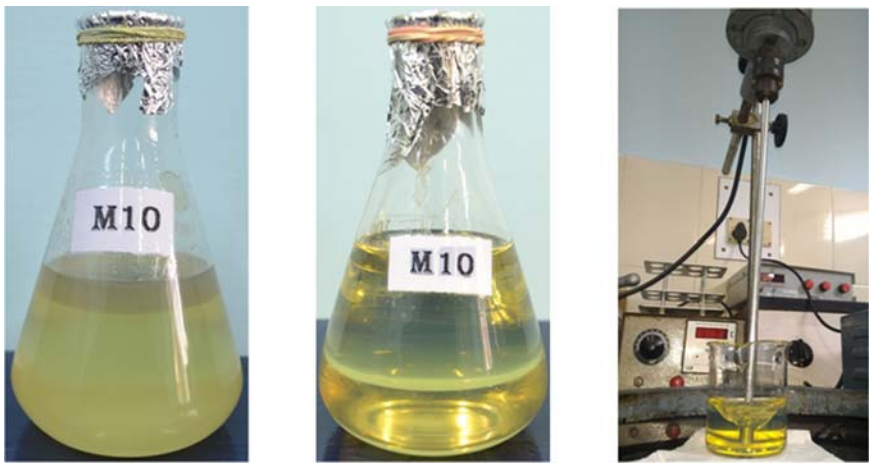

Fig. 1 Unstable MD10, stable MD10

Table 2 Technical specifications of the test engine

Engine parameters	Specifications
Make/ model	Kirloskar Oil Engines Limited, Pune, India/ DM-10
Engine type	Vertical, four-stroke, single-cylinder, constant-speed, direct-injection CI engine
Rated power output	7.4 kW (10 hp)
Rated engine speed	1500 rpm
Bore/ stroke	102 mm/ 116 mm
Displacement volume	948 cc
Compression ratio	17.5
Nozzle opening pressure	200 bars
Cooling type	Water cooling
Governor type	Mechanical, centrifugal (A2 class)

Table 3 Accuracies of the measurement equipment and experimental uncertainties

Instrument	Parameter	Accuracy
Piezoelectric pressure transducer	In-cylinder pressure	±25 pC/ bar
Exhaust gas emission analyzer	CO	±0.01% (v/v)
	HC	±1 ppm
	NOx	±1 ppm
Portable density meter	Density	±0.001 g/cm^3
Kinematic viscometer	Kinematic viscosity	±0.07%
Bomb calorimeter	Calorific value	0.02%
Diesel engine	Load	±0.5 Nm
	Speed	±5 rpm

Table 4 Technical specifications of the EEPS [23]

Make/ model	TSI/ EEPS 3090
Particle size range	5.6–560 nm
Electrometer channels	22
Time resolution	10 Hz
Sample flow rate	10 l/ min
Operating temperature range	0–40 °C
User interface	EEPS software
Maximum concentration	#10^8 particles/cm^3

engine (Kirloskar, Pune, India; DM-10). Detailed technical specifications of the test engine are given in Table 2.

The schematic of the experimental setup is shown in Fig. 2.

For the in-cylinder pressure measurement, a piezoelectric pressure transducer (Kistler, Switzerland; 6013C) was mounted flush in the cylinder engine head. These pressure signals were amplified using a charge amplifier (Kistler, Switzerland; 6613CQO3). A high precision shaft encoder (Encoders India, Faridabad, India; ENC 58/ 6-720 ABZ/5-24V) was used for detecting the angular position of the rotating crankshaft. This shaft encoder can deliver a crank position signal in every 0.5 deg crank angle (CA). These signals from pressure transducer and shaft encoder were then used by a high-speed data combustion acquisition system (Hi-Techniques, Madison; meDAQ) for detailed engine combustion analysis. For performance and emissions characterization, engine intake airflow rate and fuel flow rate were measured. For airflow rate, a laminar flow element and a U-tube manometer were installed in the experimental setup. The pressure difference across the orifice plate was measured in terms of height difference in the U-tube manometer. For measurement of different exhaust species, a portable exhaust gas emission analyzer (Horiba, Japan; 584L) was used, which could measure CO, HC, CO_2, and NOx emission concentration in the raw exhaust gas. The accuracy of instruments used for measurement of various parameters and experimental measurement uncertainties are given in Table 3.

For particulate measurement, an Engine Exhaust Particle Sizer (EEPS) spectrometer (TSI Inc., Minnesota, USA; EEPS 3090) was used. EEPS provides high temporal resolution as well as reasonable size resolution, with multiple detectors working in parallel. EEPS can measure particle sizes from ranging from 5.6 to 560 nm with a size resolution of 16 channels per decade (a total of 32 channels), with up to a maximum concentration of #10^8 particles/cm^3 in the engine exhaust. To avoid the excessive concentration error at higher engine loads, a rotating disk thermodiluter (Matter Engineering AG, UK; MD19-2E) was used to dilute the exhaust gas before its entry into the EEPS. During the experiments, the particle number concentration of diluted exhaust was measured and a dilution factor was multiplied to calculate the actual concentration of particles in the engine exhaust emerging from the tail pipe. Technical specifications of the EEPS are given in Table 4.

Engine experiments were carried out at a constant engine speed using three different test fuels, namely, MD10, MD15, and mineral diesel. Table 5 shows important operating conditions for various experiments. At each experimental condition, the engine

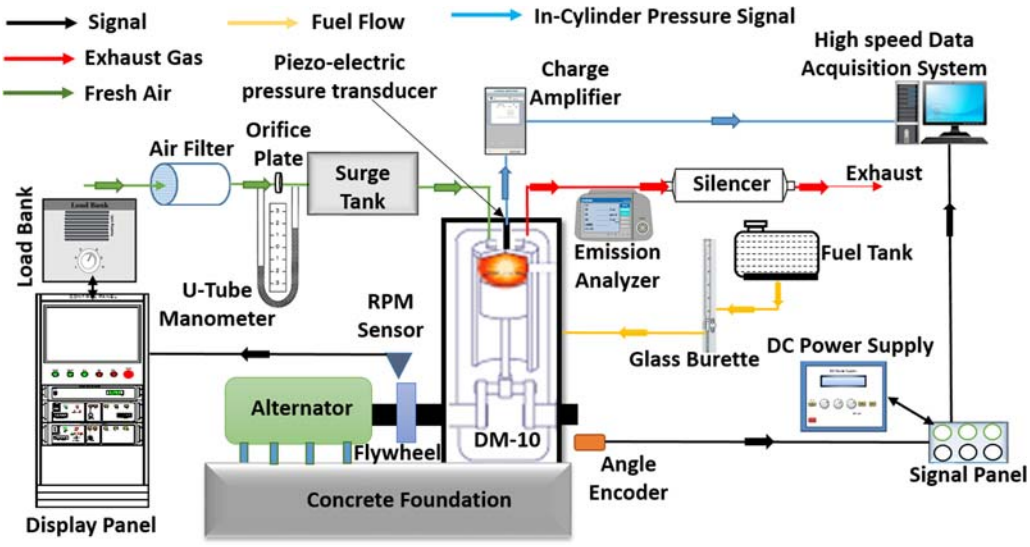

Fig. 2 Schematic of the experimental setup

Table 5 Operating conditions of the experiment

Engine speed	1500 rpm
Fuel injection pressure	200 bars
Test fuels	Diesel, MD10, and MD15
Engine load (brake mean effective pressure, BMEP)	No load, 1.25, 2.5, 3.8, and 5.0 bars

was operated for 30 min and measurements of performance, emissions, and combustion characteristics were done after thermal stabilization of the test engine.

3 Results and Discussion

3.1 Combustion Characteristics. Combustion in an engine is a rapid oxidation process, which requires specific analytical tools for its characterization. In the combustion analysis, in-cylinder pressure variations w.r.t. crank angle position play a prominent role because it provides information about different variables such as rate of pressure rise (RoPR), HRR, cumulative heat release (CHR), start of combustion (SoC), end of combustion (EoC), and CD. In-cylinder pressure was measured using a piezoelectric pressure transducer and a precision shaft encoder having a resolution of 0.5 deg CA. For all experimental conditions, in-cylinder pressure data were acquired and analyzed for a minimum of 250 consecutive engine cycles.

Figures 3(*a*)–3(*c*) show the in-cylinder pressure and RoPR variations at different engine loads for different test fuels. Engine load is expressed as brake mean effective pressure (BMEP), which is a measure of an engine's ability to do work, independent of its size. In all pressure traces, a sudden rise in in-cylinder pressure w.r.t. motoring curve represents the SoC. Results show that the SoC advanced with increasing engine load. Faster fuel-air chemical

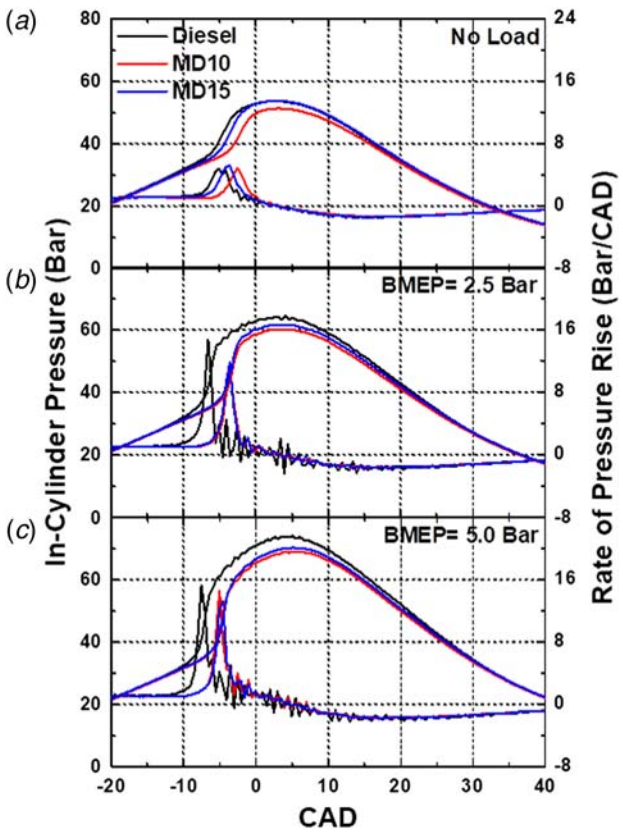

Fig. 3 In-cylinder pressure and rate of pressure rise variations w.r.t. crank angle for MD10, and MD15 vis-a-baseline mineral diesel-fueled engine at different engine loads

kinetics as well as higher in-cylinder temperature due to presence of higher fuel quantity injected may be the two factors responsible for reducing the ignition delay, leading to advanced SoC [24]. Relatively earlier SoC of mineral diesel compared with MD10 and MD15 was another important observation. The presence of methanol in mineral diesel might be a possible reason for this trend, which results in longer ignition delay (due to relatively lower cetane rating of methanol). In-cylinder charge cooling due to evaporation of methanol present in the test fuels (MD10 and MD15) also resulted in increase in ignition delay. A relative dominance of the effect of engine load over methanol blending on the ignition delay was an important observation for methanol blended gasoline. With increasing engine load, SoC of mineral diesel advanced; however, methanol–diesel blends showed a weak correlation between SoC and the engine load. At no load, SoC of MD10 was slightly earlier compared with MD15 (Fig. 3(*a*)); however at part load (BMEP = 2.5 bar) and full load (BMEP = 5.0 bar) conditions, both MD10 and MD15 exhibited almost identical SoC. Variation in fuel-air chemical kinetics of oxygenated fuel at different temperatures was the main reason for this behavior [24]. Two important radicals; "OH" and "HO_2" form during combustion and the presence of methanol affects relative concentration of these radicals in the reaction zones. Presence of methanol in the test fuels prompts the formation of H_2O_2, which is a relatively more stable radical species at lower engine loads (lower in-cylinder temperature and pressure), which results in longer ignition delay. At lower engine loads, the effect of methanol quantity was also visible on the combustion events. At higher engine loads, the effect of fuel properties was not as significant on the combustion events. This was mainly due to relatively higher in-cylinder temperature and pressure, which led to higher formation of stable H_2O_2 radicals, resulting in faster fuel-air combustion kinetics [25]. Huang et al. [14] also reported that the fraction of methanol in the test fuel did not affect the SoC significantly at higher engine loads. The slope of in-cylinder pressure curve represents the RoPR, which is calculated by differentiating the in-cylinder pressure data w.r.t. crank angle. RoPR affects the combustion noise and higher RoPR can damage the engine also in addition to deteriorating the life of engine components such as piston, connecting rod, piston rings, etc. [26]. For all test fuels, RoPR increased with increasing engine load (Fig. 3). Methanol blends exhibited slightly lower RoPR compared with baseline mineral diesel. Higher latent heat of vaporization of methanol also affected the in-cylinder thermal stratification (pressure rise), which was seen in RoPR trends (Figs. 3(*b*) and 3(*c*)) [15,27]. Results showed that RoPR increased from ~5 bar/deg CA at no load (Fig. 3(*a*)) to ~15 bar/deg CA at full load (Fig. 3(*c*)). Presence of pressure fluctuations near top dead center (TDC) in the RoPR curves hints at slight knocking. Among all test fuels, mineral diesel exhibited greater knocking compared with methanol blends. The peak of in-cylinder pressure curves showed the maximum in-cylinder pressure (P_{max}), which increased with increasing engine load. Results showed that P_{max} of mineral diesel was comparable with that of MD10 and MD15 at no load; however at higher loads, mineral diesel exhibited relatively higher P_{max} compared with methanol blends. Relatively lower in-cylinder gas temperature due to higher latent heat of vaporization and higher specific heat as well as lower heat of reaction of methanol were the main reasons for this behavior [27]. Amongst all test fuels, MD10 exhibited the lowest P_{max} compared with other test fuels.

Figures 4(*a*)–4(*c*) show HRR and CHR variations with engine load for MD10, MD15, and baseline mineral diesel. Heat release analysis was done using "zero-dimensional heat release model" [28].

Increasing engine load resulted in higher HRR. Comparison of HRR curves of different test fuels showed that mineral diesel exhibited slightly higher HRR compared with methanol blends (Figs. 4(*b*) and 4(*c*)). Relatively higher calorific value of mineral diesel compared with MD10 and MD15 may be a possible reason for this trend (Table 1). The width of HRR curve peak shows "premixed combustion" phase. Figure 4 shows that increasing engine

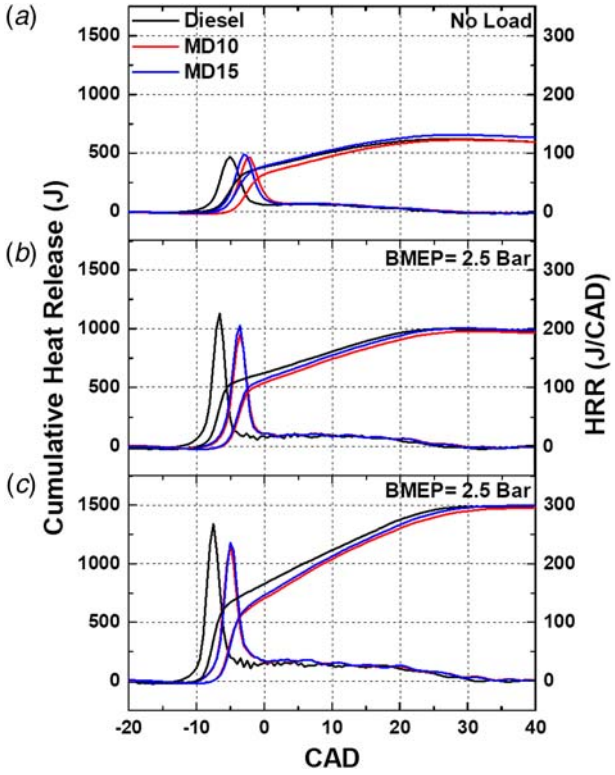

Fig. 4 HRR and CHR variations w.r.t. CAD for MD10, MD15, and mineral diesel-fueled engine at different engine loads

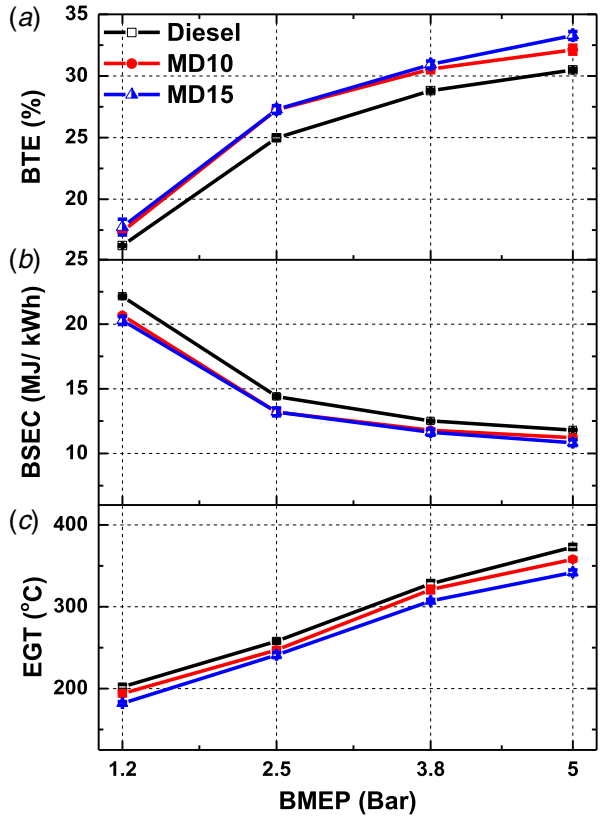

Fig. 5 BTE, BSEC, and EGT of MD10, MD15, and mineral diesel-fueled engine at different engine loads

load resulted in shorter premixed combustion duration, which was also visible in the RoPR trends (Fig. 3). HRR trends showed that increasing engine load mainly affected the HRR trends in the "diffusion combustion" phase. At higher engine loads, the quantity of methanol injected in the combustion chamber also increased because of higher total fuel quantity injected. This resulted in relatively slower fuel-air combustion kinetics, leading to relatively longer combustion duration (Figs. 4(*b*) and 4(*c*)). This was also observed in the HRR trends also, which showed dominant "diffusion (slow) combustion" phase at higher engine loads. Presence of higher in-cylinder pressure and temperature converted the inactive H_2O_2 radicals into active OH radicals, which accelerated the combustion speed, increased the intensity of "diffusion combustion" phase and thus shortened the combustion duration [25]. At higher engine loads, HRR trends of MD10 and MD15 were similar, which showed that the amount of methanol blended with mineral diesel at higher engine loads did not affect the combustion significantly.

To analyze the overall combustion quality, CHR analysis was also carried out. The slope of CHR curve showed the HRR, and the height of the CHR curve shows the total heat released during an engine cycle (Figs. 4(*a*)–4(*c*)). CHR trends showed that heat released during premixed combustion increased with increasing engine load; however, increase in heat release during the diffusion combustion phase was more dominant compared with the premixed combustion phase (Figs. 4(*b*) and 4(*c*)). At no engine load, CHR was ~600 kJ/m^3, in which ~35% energy was released during diffusion combustion phase (Fig. 4(*a*)); however at full engine load, CHR was ~1500 kJ/m^3, in which ~66% energy was released during the diffusion combustion phase (Fig. 4(*c*)). CHR trends of different test fuels were different at lower engine loads; however, these differences reduced with increasing engine load. CHR analysis also exhibited relatively slower heat release from MD10 and MD15 during premixed combustion phase; however at the end of the cycle, all test fuels showed almost similar CHR. Among all test fuels, MD10 showed slightly lower CHR compared with MD15 and mineral diesel.

3.2 Performance and Emission Characteristics. Experiments were conducted to characterize engine performance parameters, namely, BTE, brake-specific energy consumption (BSEC), and exhaust gas temperature (EGT) w.r.t. engine load.

Figure 5(*a*) shows the effect of methanol addition to mineral diesel on BTE, which increases with increasing engine load for all test fuels. MD15 and MD10 showed relatively higher BTE compared with baseline mineral diesel. Bayraktar [9], Huang et al. [14], and Jamrozik [12] also reported higher BTE for methanol–diesel blends compared with mineral diesel. Retarded combustion phasing, higher flame speed, shorter combustion duration, and presence of fuel bound oxygen during combustion of MD10 and MD15 were the possible reasons for this trend [26,28]. Higher evaporative charge cooling (due to higher latent heat of vaporization of methanol) resulted in lower temperatures at the end of the compression stroke, which reduced the required work input to the compression stroke and contributed to higher BTE of MD10 and MD15. Lean-burn operation of methanol due to its wider flammability limit might be another possible reason for higher BTE for methanol–diesel blends. The difference among the test fuels was slightly higher at higher engine loads, where all the above mentioned factors were more dominant compared with lower engine loads. Figure 5(*b*) shows that the BSEC of mineral diesel was relatively higher compared with MD10 and MD15. BSEC of both the oxygenated test fuels were almost similar. Figure 5(*c*) shows the variations in EGT for MD10, MD15, and mineral diesel-fueled engine at different engine loads. EGT was an indirect measure of in-cylinder temperature, which showed an increasing trend with increasing engine load. Among all test fuels, mineral diesel fueled engine resulted in relatively higher EGT compared with MD10 and MD15. Higher latent heat of vaporization of methanol compared with mineral diesel may be an important factor behind the lower EGT of methanol blends, which reduced the in-cylinder gas temperature.

To compare the emission characteristics of MD10, MD15, and mineral diesel-fueled engines, brake-specific emissions of CO, HC, and NOx were measured and analyzed at all engine loads. Brake-specific mass emissions were calculated from the measured species concentrations in the engine exhaust using intake airflow rate, fuel flow rate, and power output data [29]. Figure 6(*a*) shows the comparison of CO emitted by oxygenated test fuels compared with baseline mineral diesel. CO is a toxic by-product of incomplete combustion of hydrocarbon fuels. CO emission depends on several factors such as engine load, presence of oxygen, etc. At lower engine loads, all test fuels emitted higher CO, which decreased with increasing engine load [20]. Presence of lower in-cylinder temperature was the main reason for this, which prevented oxidation of CO into CO_2. At higher engine loads, lack of oxygen hampered the oxidation of CO into CO_2, resulting in slightly higher CO emission. Figure 6(*a*) clearly depicted that methanol blended mineral diesel resulted in lower CO emission compared with baseline mineral diesel. Among all test fuels, MD15 exhibited the lowest CO emission at all loads. Presence of fuel bound oxygen in methanol–diesel blends resulted in leaner combustion, which allowed the presence of higher oxygen in the combustion gases. This led to greater conversion of CO into CO_2 compared with baseline mineral diesel, therefore leading to lower CO emission.

Figure 6(*b*) shows the comparison of HC emissions from MD10, MD15, and mineral diesel at different engine loads. HC emissions are also a consequence of incomplete combustion of hydrocarbon fuels. At lower engine loads, lower peak in-cylinder temperature led to higher HC emissions, which decreased with increasing engine load. Faster fuel-air chemical kinetics and higher in-cylinder temperature may be possible reasons for lower HC emissions at higher engine loads. Among all test fuels, methanol–diesel blends resulted in relatively lower HC emissions compared with baseline mineral diesel. Increase in the flame speed due to the presence of methanol in mineral diesel may be another reason for lower HC emissions, which reduced the combustion duration and increased the in-cylinder combustion temperature. Higher combustion temperature promoted more complete combustion, leading to lower HC emissions. Participation of fuel bound oxygen in methanol–diesel blends improved the degree of completion of combustion. Sayin et al. [10] and Canacki et al. [13] also observed similar CO and HC emission trends.

Figure 6(*c*) shows the comparison of NOx emitted from MD10, MD15, and mineral diesel-fueled engine at different engine loads. NOx formation is affected by three parameters: oxygen concentration in the test fuel, peak combustion temperature, and time availability because NOx formation involves hundreds of elementary chemical reactions. In general, NOx emissions increased with increasing engine load. However, due to the combined effect of all factors, NOx emissions showed a random pattern with increasing engine load. For mineral diesel and MD10, NOx emissions slightly decreased with increasing engine load; however for MD15, NOx emissions first increased and then decreased. The cooling effect of methanol due to higher latent heat lowered the in-cylinder combustion temperature hence reduced the NOx formation. However, oxygen content in the test fuel increased the fuel oxygen availability in the reaction zone, which increased the NOx formation. Among all test fuels, MD15 showed the lowest NOx emissions. MD10 and mineral diesel showed almost comparable NOx emissions. In MD15, cooling effect of methanol dominated over the fuel oxygen availability; however in case of MD10, oxygen availability dominated over the in-cylinder cooling effect due to higher latent heat of vaporization. Previous literature also presented similar results as Huang et al. [30], who reported both increased and decreased NOx emissions; Chao et al. [31] reported reduction, and Popa et al. [32] reported increased NOx emissions due to the presence of methanol in mineral diesel.

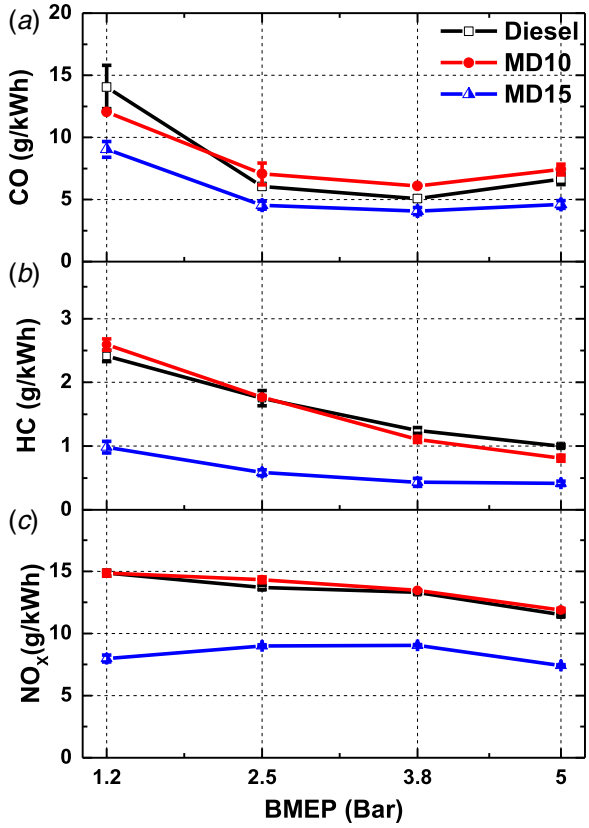

Fig. 6 CO, HC, and NOx emitted by MD10, MD15, and mineral diesel-fueled engine at different loads

3.3 Particulate Characteristics. Particulate from diesel engines are a result of heterogeneous combustion, which generates soot precursors in oxygen-deficient regions of the combustion chamber. High in-cylinder temperature and pressure conditions post-combustion promote the growth of existing soot nuclei [33]. All these processes related to particulate formation are significantly affected by fuel properties, fuel composition, and engine combustion characteristics. Therefore, an important aspect of this study is to look at particulate emissions from methanol–diesel blend fueled CI engine comprehensively.

For better understanding, Fig. 7 is split into three parts, namely, number–size, surface area–size, and mass–size distributions of particulates emitted by MD10, MD15, and mineral diesel-fueled engine at a medium load of 2.5 bars BMEP. Experimental results showed that the mineral diesel-fueled engine emitted a relatively higher number of particulates in the entire size range compared with methanol–diesel blends. Relatively longer ignition delay of MD10 and MD15 was an important reason for lower particulate emissions. Due to longer ignition delay of methanol–diesel blends, more fuel quantity was burnt in the "premixed combustion phase" and lower fuel quantity burnt in the "diffusion combustion phase," which was responsible for lower particulate formation compared with baseline mineral diesel. Mineral diesel-fueled engine showed a wider number–size distribution of particulates compared with methanol–diesel blends. The difference between the particulates emitted by mineral diesel, MD10, and MD15 fueled engines were relatively smaller in the medium-size range ($30\ \text{nm} < D_p < 80\ \text{nm}$). Fuel oxygen present in methanol–diesel blends reduced formarion of soot precursors in the fuel-rich zone due to an increased concentration of O and OH radicals, which promoted oxidation of soot precursors to CO and CO_2. Higher concentration of OH radicals generated during combustion of methanol–diesel blends also limited the formation of aromatic rings as well as soot nucleation [25]. Reduction of carbon content in the methanol–diesel blends (due to lower C/H ratio) led to lower number of

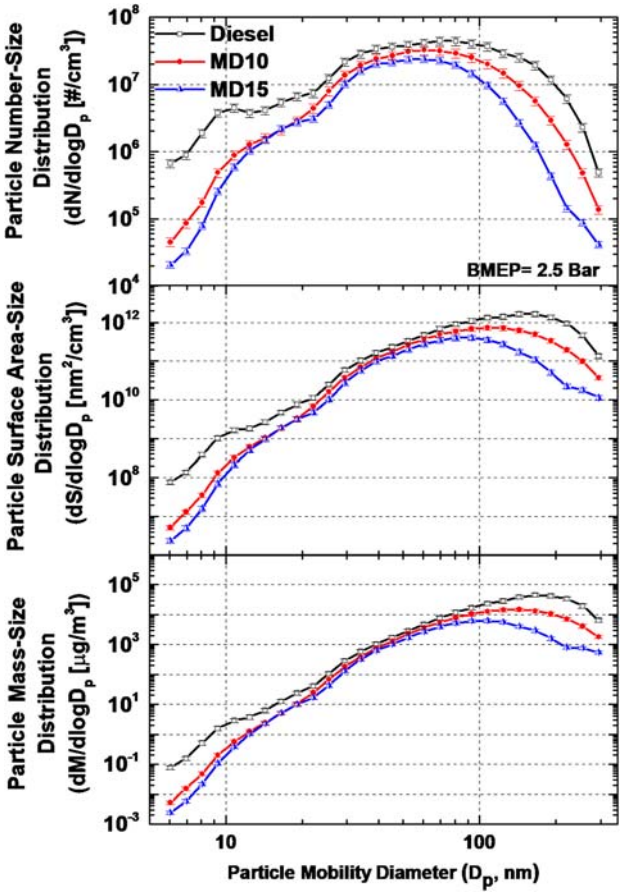

Fig. 7 Number–size distribution, surface area–size distribution, and mass–size distribution of particulates emitted by MD10, MD15, and mineral diesel-fueled engine at medium engine load (BMEP: 2.5 bars)

particulate formation compared to mineral diesel fueled-engine. These factors might be responsible for a greater difference between the number concentration of smaller particulates ($D_p <$ 30 nm) emitted by mineral diesel and methanol–diesel blends fueled engines. Improved fuel spray atomization characteristics of methanol–diesel blends compared with mineral diesel improved the combustion, which slowed down the coagulation and agglomeration of small particulates into larger particulates [34]. Due to improved combustion, the tendency of condensation of volatile species also reduced, which resulted in a higher difference in number concentration of bigger particles ($D_p > 80$ nm) emitted by the mineral diesel and methanol–diesel blend fueled engine.

Particle surface area is another important parameter, which directly influences the toxicity of particulates. Particle surface area was calculated by assuming exhaust particulates to be perfectly spherical [23].

$$dS = dN.(D_p)^2$$

where dS is the area concentration of size range with mean diameter D_p and dN is the number concentration of particulates with mean diameter D_p. Figure 7 shows that the surface area of particulates emitted by oxygenated fuels was relatively lower compared with baseline mineral diesel. With increasing oxygen content of the test fuels, particulate surface area decreased. This shows that particulates emitted from MD15 have a lesser tendency to adsorb polycyclic aromatic hydrocarbons (PAHs), hence they may be less toxic compared with baseline mineral diesel origin particulates.

Particulate mass–size distribution is another important aspect of this study. Particulate mass was calculated directly from particle volume, assuming that the particle density does not vary with changing size of the emitted particulates from the engine tailpipe [23]. Particle volume/mass directly affects the particle life in the atmosphere because bigger particles have relatively higher mass; therefore, the possibility of their settling down is also higher since heavier particles tend to settle faster. Lower mass particles, i.e., smaller particles have higher ambient retention time compared with larger mass particles or larger particles. This can be directly correlated with the exposure time since smaller particles have a higher probability to be inhaled in the human body. Figure 7 shows that oxygenated fuels emitted significantly lower particulate mass compared with baseline mineral diesel. With increasing oxygen content in the test fuels, particulate mass reduced due to superior oxidation of test fuels. Among all test fuels, MD15 resulted in the lowest particulate mass (an order lower compared with mineral diesel) emission.

Figure 8 shows the particle number concentration based on their size range, namely, nucleation mode particles (NMP, $D_p < 50$ nm), accumulation mode particles (AMP, 50 nm $< D_p <$ 1000 nm), and total particle number (TPN). This analysis shows the effectiveness of methanol addition in mineral diesel for particulate emission reduction on different size ranges. Results showed that addition of methanol to mineral diesel reduced both NMP and AMP. MD10 showed ~35% reduction in NMP and ~43% reduction in AMP number concentrations, and MD15 showed ~50% reduction in NMP and ~68% reduction in AMP number concentration compared with baseline mineral diesel. MD15 resulted in almost equal number concentration of NMP and AMP; however in case of mineral diesel, AMP number concentration was significantly higher compared with NMP number concentration.

Figure 9 shows the correlation between TPN, total particle mass (TPM), and count mean diameter (CMD) of particulates emitted by MD10, MD15, and mineral diesel. CMD represents the number weighted arithmetic average of particulate size. CMD was calculated using the following equation.

$$\text{CMD} = \frac{n_1 d_1 + n_2 d_2 + n_3 d_3 + \cdots\cdots + n_n d_n}{n_1 + n_2 + n_3 + \cdots\cdots + n_n}$$

where n_i is the particle number concentration corresponding to the diameter d_i.

Among all test fuels, MD15 showed the lowest TPM and TPN followed by MD10. Mineral diesel-fueled engine resulted in highest TPN and TPM. Due to relatively smaller particulates emitted by MD10 and MD15 fueled engine, CMD of these particulates was also relatively lower compared with mineral diesel. Particulates having smaller CMD represent a higher probability to be inhaled deeper into the lungs. However, the overall analysis

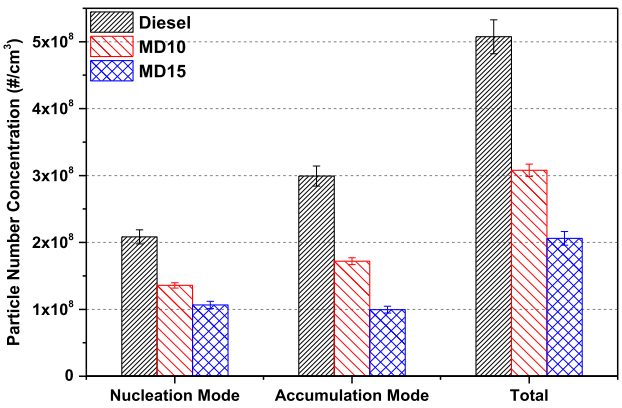

Fig. 8 Nucleation mode, accumulation mode, and total number concentration of particulates emitted by MD10, MD15, and mineral diesel-fueled engine at medium engine load (BMEP: 2.5 bars)

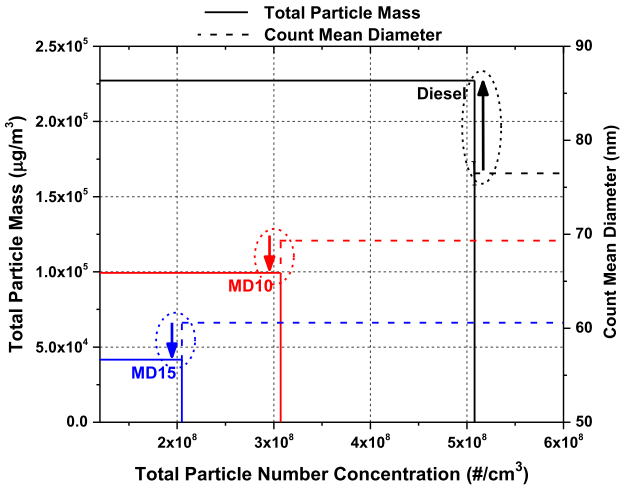

Fig. 9 Correlation between total particle number, total particle mass, and count mean diameter of particles emitted by MD10, MD15, and mineral diesel-fueled engine at medium engine load (BMEP: 2.5 bars)

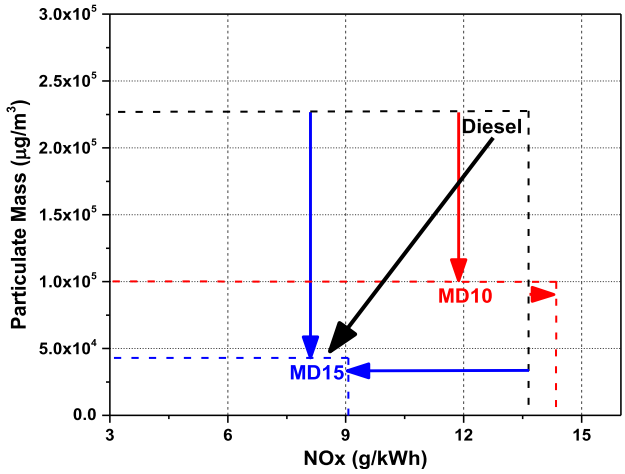

Fig. 11 Effectiveness of methanol blending with mineral diesel for emission reduction (particulate and NOx) at medium engine load (BMEP: 2.5 bars)

suggests that particulates from mineral diesel were more harmful due to their higher TPN and TPM (Fig. 9).

Figure 10 shows the correlation between particle number and mass emissions. The inclination of dome toward particle mass axis signifies dominant mass emissions, and inclination of dome toward particle number axis signifies dominant particle number emissions [35]. Figure 10 shows that the mineral diesel-fueled engine emitted particulate with higher in number as well as in mass. However, particulates emitted by MD10 and MD15 fueled engine were more inclined toward number axis, which suggests that methanol addition to mineral diesel resulted in a higher number of particulates of relatively smaller size. These particulates did not contribute significantly to the particulate mass. Overall, it can be stated that the addition of oxygenated fuel such as methanol to mineral diesel reduced the particulate mass emission by reducing the rate of coagulation and agglomeration.

Figure 11 shows the NOx-TPM trade-off analysis, which is the most critical issue for internal combustion (IC) engines, especially for CI engines [36–39]. This analysis showed that the addition of methanol to mineral diesel certainly reduced the particulate emissions; however, NOx emissions reduced only in case of MD15. Presence of lower methanol content in mineral diesel (10% v/v) resulted in superior oxidation of test fuel into CO and CO_2; however, the presence of fuel oxygen also increased the NOx emissions slightly. Presence of higher methanol content in mineral diesel (15% v/v) resulted in improved oxidation as well as lean-burn combustion in addition to dominant in-cylinder charge cooling effect, which reduced both NOx and TPM emissions simultaneously. This reflected that a certain minimum methanol content (15% v/v) should be added to mineral diesel in order to reduce both NOx and PM emissions from CI engines simultaneously.

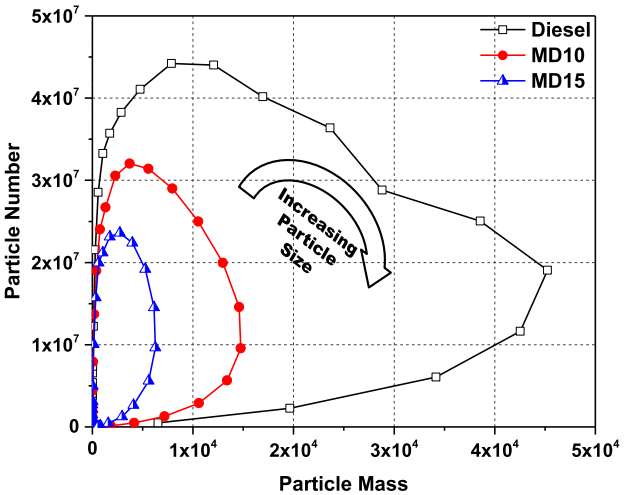

Fig. 10 Correlation between number–size and mass–size distributions of particulates emitted by MD10, MD15, and mineral diesel-fueled engine at medium engine load (BMEP: 2.5 bars)

Conclusions

In this study, a comprehensive set of experiments were conducted to understand the combustion, performance, gaseous emissions, and particulate emission characteristics of a constant speed single-cylinder genset engine using methanol–diesel blends (MD10 and MD15) vis-à-vis baseline mineral diesel. It was found that lower methanol-mineral diesel blend with an additive (1% v/v dodecanol) can be used in unmodified genset engines. Combustion investigation showed that the addition of methanol to mineral diesel did not affect engine combustion characteristics significantly. Methanol blended with mineral diesel showed relatively smoother combustion compared with baseline mineral diesel at higher engine loads. Slightly retarded combustion of MD10 and MD15 was another important observation. Among all test fuels, MD15 exhibited higher BTE, lower BSEC, and lower HC, CO, and NOx emissions. Particulate investigations showed that MD10 and MD15 fueled engines emitted lesser number of particulates and lower particulate mass compared with baseline mineral diesel. MD15 reduced both NOx and particulate emissions simultaneously. Overall, this experimental study established the technical feasibility of using methanol–diesel blends in unmodified genset CI engines with acceptable engine combustion, performance, and emission characteristics. MD15 emerged to be a technically feasible blend for large-scale implementation of methanol in CI engines and exhibited superior performance and emission characteristics compared with baseline mineral diesel, without the need for any significant hardware modifications in the engines used in agricultural and decentralized power generation sectors.

References

[1] Agarwal, A. K., Singh, A. P., and Maurya, R. K., 2017, "Evolution, Challenges and Path Forward for Low Temperature Combustion Engines," Prog. Energy Combust. Sci., **61**, pp. 1–56.

[2] Singh, A. P., and Agarwal, A. K., 2017, "Partially Homogenous Charge Compression Ignition Engine Development for Low Volatility Fuels," Energy Fuels, **31**(3), pp. 3164–3181.

[3] Agarwal, A. K., Agarwal, A., and Singh, A. P., 2015, "Time Resolved In-Situ Biodiesel Combustion Visualization Using Engine Endoscopy," Measurement, **69**, pp. 236–249.
[4] Singh, A. P., Pal, A., and Agarwal, A. K., 2016, "Comparative Particulate Characteristics of Hydrogen, CNG, HCNG, Gasoline and Diesel Fueled Engines," Fuel, **185**, pp. 491–499.
[5] Singh, A. P., and Agarwal, A. K., 2017, "CI/PCCI Combustion Mode Switching of Diesohol Fuelled Production Engine," SAE Technical Paper, Paper No. 2017-01-0738.
[6] Agarwal, A. K., 2007, "Biofuels (Alcohols and Biodiesel) Applications as Fuels in Internal Combustion Engines," Prog. Energy Combust. Sci., **32**(3), pp. 233–271.
[7] Nord, A. J., Hwang, J. T., and Northrop, W. F., 2017, "Emissions From a Diesel Engine Operating in a Dual-Fuel Mode Using Port-Fuel Injection of Heated Hydrous Ethanol," ASME J. Energy Resour. Technol., **139**(2), p. 022204.
[8] ManiSarathy, S., Oßwald, P., Hansen, N., and Kohse-Höinghaus, K., 2014, "Alcohol Combustion Chemistry," Prog. Energy Combust. Sci., **44**, pp. 40–102.
[9] Bayraktar, H., 2008, "An Experimental Study on the Performance Parameters of an Experimental CI Engine Fueled With Diesel–Methanol–Dodecanol Blends," Fuel, **87**(2), pp. 158–164.
[10] Sayin, C., Ozsezen, A. N., and Canakci, M., 2010, "The Influence of Operating Parameters on the Performance and Emissions of a DI Diesel Engine Using Methanol-Blended-Diesel Fuel," Fuel, **89**(7), pp. 1407–1414.
[11] Yilmaz, N., and Donaldson, A. B., 2007, "Modeling of Chemical Processes in a Diesel Engine With Alcohol Fuels," ASME J. Energy Resour. Technol., **129**(4), pp. 355.
[12] Jamrozik, A., 2017, "The Effect of the Alcohol Content in the Fuel Mixture on the Performance and Emissions of a Direct Injection Diesel Engine Fueled With Diesel-Methanol and Diesel-Ethanol Blends," Energy Convers. Manage., **148**, pp. 461–476.
[13] Canakci, M., Sayin, C., Ozsezen, A. N., and Turkcan, A., 2009, "Effect of Injection Pressure on the Combustion, Performance, and Emission Characteristics of a Diesel Engine Fueled With Methanol-Blended Diesel Fuel," Energy Fuels, **23**(6), pp. 2908–2920.
[14] Huang, Z., Lu, H., Jiang, D., Zeng, K., Liu, B., and Zhang, J., 2004, "Engine Performance and Emissions of a CIengine Operating on the Diesel-Methanol Blends," Proc. Inst. Mech. Eng. Part D, **218**(4), pp. 435–447.
[15] Agarwal, A. K., Shukla, P. C., Patel, C., Gupta, J. G., Sharma, N., Prasad, R. K., and Agarwal, R. A., 2016, "Unregulated Emissions and Health Risk Potential From Biodiesel (KB5, KB20) and Methanol Blend (M5) Fuelled Transportation Diesel Engines," Renew. Energy, **98**, pp. 283–291.
[16] Wei, H., Yao, C., Pan, W., Han, G., Dou, Z., Wu, T., Liu, M., Wang, B., Gao, J., Chen, C., and Shi, J., 2017, "Experimental Investigations of the Effects of Pilot Injection on Combustion and Gaseous Emission Characteristics of Diesel/Methanol Dual Fuel Engine," Fuel, **188**, pp. 427–441.
[17] Wu, H., Fan, C., He, J., and Hsu, T., 2017, "Optimal Factors Estimation for Diesel/Methanol Engines Changing Methanol Injection Timing and Inlet Air Temperature," Energy, **141**, pp. 1819–1828.
[18] Yao, C., Hu, J., Geng, P., Shi, J., Zhang, D., and Ju, Y., 2017, "Effects of Injection Pressure on Ignition and Combustion Characteristics of Diesel in a Premixed Methanol/air Mixture Atmosphere in a Constant Volume Combustion Chamber," Fuel, **206**, pp. 593–602.
[19] Chen, Z., Yao, C., Wang, Q., Han, G., Dou, Z., Wei, H., Wang, B., Liu, M., and Wu, T., 2016, "Study of Cylinder-to-Cylinder Variation in a Diesel Engine Fueled With Diesel/Methanol Dual Fuel," Fuel, **170**, pp. 67–76.
[20] Venkataraman, C., and Rao, G. U. M., 2001, "Emission Factors of CarbonMonoxide and Size-ResolvedAerosols From Biofuel Combustion," Environ. Sci. Technol., **35**, pp. 2100–2107.
[21] Shamun, S., Haşimoğlu, C., Murcak, A., Andersson, Ö, Tunér, M., and Tunestål, P., 2017, "Experimental Investigation of Methanol Compression Ignition in a High Compression Ratio HD Engine Using a Box-Behnken Design," Fuel, **209**, pp. 624–633.
[22] Murayama, T., Miyamoto, N., Yamada, T., Kawashima, J. I., and Itow, K., 1982, "A Method to Improve the Solubility and Combustion Characteristics of Alcohol-Diesel Fuel Blends," SAE Technical Paper, Paper No. 821113.
[23] Engine Exhaust Particle Sizer™ Spectrometer Model 3090, Operation and Service Manual, TSI, March 2009.
[24] Yin, Z. H., Yao, C. D., Geng, P. L., and Hu, J. T., 2016, "Visualization of Combustion Characteristic of Diesel in Premixed Methanol-Air Mixture Atmosphere of Different Ambient Temperature in a Constant Volume Chamber," Fuel, **174**, pp. 242–250.
[25] Chen, H., Su, X., He, J., and Xie, B., 2019, "Investigation on Combustion and Emission Characteristics of a Common Rail Diesel Engine Fueled With Diesel/n-Pentanol/Methanol Blends," Energy, **167**, pp. 297–311.
[26] Singh, A. P., and Agarwal, A. K., 2012, "Combustion Characteristics of Diesel HCCI Engine: An Experimental Investigation Using External Mixture Formation Technique," Appl. Energy, **99**, pp. 116–125.
[27] Singh, A. P., and Agarwal, A. K., 2016, "Diesoline, Diesohol, and Diesosene Fuelled HCCI Engine Development," ASME J. Energy Resour. Technol., **138**(5), pp. 052212.
[28] Heywood, J. B., 1988, *Internal Combustion Engine Fundamentals*, McGraw-Hill, New York.
[29] Indian Standard IS: 14273, 1999, *Automotive Vehicles—Exhaust Emissions—Gaseous Pollutants From Vehicles Fitted With Compression Ignition Engines—Method of Measurement*, Bureau of Indian Standards, New Delhi, India.
[30] Huang, Z. H., Lu, B. H., Jiang, D. M., Zeng, K., Liu, B., and Zhang, J. Q., 2004, "Combustion Characteristics and Heat Release Analysis of a Compression Ignition Engine Operating on a Diesel/Methanol Blend," Proc. Inst. Mech. Eng. Part D: J. Automob. Eng., **218**(4), pp. 435–447.
[31] Chao, M. R., Lin, T. C., Chao, H. R., Chang, F. H., and Chen, C. B., 2001, "Effect of Methanol-Containing Additive on the Emission Characteristics From a Heavy-Duty Diesel Engine," Sci. Total Environ. **279**(1–3), pp. 167–179.
[32] Popa, M. G., Negurescu, N., Pana, C., and Racovitza, A., 2001, "Results Obtained by Methanol-Fueling Diesel Engine," SAE Technical Paper, No. 2001-01-3748.
[33] Agarwal, A. K., Singh, A. P., Lukose, J., and Gupta, T., 2013, "Characterization of Exhaust Particulates From Diesel Fueled Homogenous Charge Compression Ignition Combustion Engine," J. Aerosol Sci., **58**, pp. 71–85.
[34] Zhu, R., Cheung, C. S., and Huang, Z., 2011, "Particulate Emission Characteristics of a Compression Ignition Engine Fueled with Diesel–DMC Blends," Aerosol Sci. Technol., **45**(2), pp. 137–147.
[35] Shukla, P. C., Gupta, T., Gupta, N., and Agarwal, A. K., 2017, "A Qualitative Correlation Between Engine Exhaust Particulate Number and Mass Emissions," Fuel, **202**, pp. 241–245.
[36] Jain, A., Singh, A. P., and Agarwal, A. K., 2017, "Effect of Split Fuel Injection and EGR on NOx and PM Emission Reduction in a Low Temperature Combustion (LTC) Mode Diesel Engine," Energy, **122**, pp. 249–264.
[37] Maurya, R. K., and Agarwal, A. K., 2015, "Experimental Investigations of Particulate Size and Number Distribution in an Ethanol and Methanol Fueled HCCI Engine," ASME J. Energy Resour. Technol., **137**(1), pp. 12201.
[38] Agarwal, A. K., Park, S., Dhar, A., Lee, C. S., Park, S., Gupta, T., and Gupta, N. K., 2018, "Review of Experimental and Computational Studies on Spray, Combustion, Performance, and Emission Characteristics of Biodiesel Fueled Engines," ASME J. Energy Resour. Technol., **140**(12), pp. 120801.
[39] Singh, A. P., and Agarwal, A. K., 2018, "Low Temperature Combustion Engines and Mode Switching Strategies—A Review," J. Energy Environ. Sustainability, **6**, pp. 42–47.